Order-Reduction of Parabolic PDEs with Time-Varying Domain Using Empirical Eigenfunctions

Mojtaba Izadi and Stevan Dubljevic
Dept. of Chemical and Materials Engineering, University of Alberta, Edmonton, AB, Canada, T6G 2V4

DOI 10.1002/aic.14152
Published online June 24, 2013 in Wiley Online Library (wileyonlinelibrary.com)

A novel methodology for the order-reduction of parabolic partial differential equation (PDE) systems with time-varying domain is explored. In this method, a mapping functional is obtained, which relates the time-evolution of the solution of a parabolic PDE with time-varying domain to a fixed reference domain, while preserving space invariant properties of the initial solution ensemble. Subsequently, the Karhunen–Loève decomposition is applied to the solution ensemble on fixed spatial domain resulting in a set of optimal eigenfunctions. Further, the low dimensional set of empirical eigenfunctions is mapped on the original time-varying domain by an appropriate mapping, resulting in the basis for the construction of the reduced-order model of the parabolic PDE system with time-varying domain. This methodology is used in three representative cases, one- and two-dimensional (1-D and 2-D) models of nonlinear reaction-diffusion systems with analytically defined domain evolutions, and the 2-D model of the Czochralski crystal growth process with nontrivial geometry. © 2013 American Institute of Chemical Engineers *AIChE J*, 59: 4142–4150, 2013
Keywords: modeling and order reduction of distributed parameter systems, reaction-diffusion, (conduction) parabolic PDEs model reduction, time-varying processes, Karhunen-Loeve decomposition, Czochralski crystal growth process

Introduction

The modeling of a transport process is the most important issue in the process analysis and control design. It is currently addressed by phenomenological modeling arising from theoretical first-principles, experimental studies and/or with the help of the system identification theory. In many industries including chemical, petrochemical, and pharmaceutical plants, model-based control has been very successful; in majority of them, the underlying plant model is low-dimensional and linear. In general, mathematical models of many industrial relevant transport processes are obtained from conservation laws, such as mass, momentum and/or energy, and yield the forms given by nonlinear partial differential equations (PDEs). In addition, many of these processes involve a change in shape and material properties which can be characterized by phenomena associated with the phase change, generation and consumption of chemical species through the chemical reaction mechanism, heat and mass transfer.

In the past, dynamical analysis and control of parabolic PDEs with fixed spatial domain have been studied extensively, though, few investigations are available for the systems with time-dependent spatial domains. From the control point of view, main contributions include Wang's work on the stabilization and optimal control problem of such systems[1] and application in the synthesis of linear optimal controller for thermal gradient regulation in crystal growth processes,[2] and Ray and Seinfeld's[3] study on the design of nonlinear distributed state estimators using stochastic methods. More recently, Ng and Dubljevic posed the time-varying optimal control problem[4] and boundary control formulation[5] for regulation of a parabolic PDE with time-varying domain by representing the PDE as an abstract evolution equation on an infinite-dimensional function space with nonautonomous parabolic operator which generates a two-parameter semigroup.

Low-dimensional model identification of distributed parameter systems governed by nonlinear PDEs attracted attention of a significant number of researchers in recent years. Among many, the most notable contributions came from Ray and coworkers,[6,7] Park and Cho,[8] Christofides and coworkers,[9,10] and Hoo and coworkers.[11,12] In these contributions, the common interpretation is that the dissipative distributed parameter systems could be modeled and reduced to a low finite-dimensional system representation which captures the dominant dynamics, while the infinite-dimensional complement associated with the fast and stable dynamics can be neglected. The similar conceptual representation appears in the hydrodynamics where "coherent structures" are associated with the most dominant modes.[13,14]

In general, the model order-reduction can be achieved through the Galerkin's method which assumes the exact knowledge of the model and requires an analytic solution for the eigenvalue problem associated with the nonlinear spatial operator of a parabolic PDE. However, there is no general analytic solution to the operator eigenvalue problem, examples are the nonlinear spatial operator or problems with nontrivial geometric domain. In such cases, the exact description of the underlying distributed parameter system is not known,

Correspondence concerning this article should be addressed to S. Dubljevic at stevan.dubljevic@ualberta.ca.

so the input–output model order-reduction approach has been proposed and explored.[6] A well-known approach in the extraction of spatial characteristics (modes) of distributed parameter systems is the use of Karhunen–Loève (KL) expansion on an ensemble of solutions obtained from numerical or experimental resolution of the system.[8] These modes, known as empirical eigenfunctions, are used as the basis set of functions in the Galerkin's method. This approach is widely used in the derivation of accurate reduced-order approximations of many diffusion-reaction systems and fluid flows.

Bangia et al.[15] used KL to find the eigenfunctions of accurate numerical solutions of the Navier–Stokes equations to study the bifurcation of incompressible flow in a model complex geometry. Park and Cho applied KL decomposition to a nonlinear two-dimensional (2-D) heat conduction problem with a nontrivial domain to obtain the reduced-order model.[8] In other contributions, Park and coworkers used KL method to find basis functions for Galerkin's method to solve the inverse forced[13] and natural[16] convection problems. In Refs. 17–19, low-dimensional models for specific diffusion-reaction systems are obtained using empirical eigenfunctions as basis functions in Galerkin's method, which is used to synthesize linear and nonlinear feedback controllers.

Other applications include, but are not limited to, the order-reduction of the sheet-forming processes,[20] order-reduction and control of multiscale model of microstructure of materials during epitaxial growth,[21] optimal control of batch electrochemical reactor,[22] order-reduction of the nonlinear model of molten carbonate fuel cell,[23] order-reduction and regulation of thermal transients in microsystem models,[24] order-reduction of multiscale thermal model for electronic cabinets,[25] ground-water flow model reduction,[26] and order-reduction of low-voltage cascade electro-osmotic micro-pump model.[27]

Compared to the aforementioned extensive research efforts toward identification and model reduction of distributed parameter systems modeled by parabolic PDEs, there are only few studies to address order-reduction of parabolic PDE systems with spatial time-varying domain. In a series of works, Armaou and Christofides[28] used a mathematical transformation to represent the nonlinear parabolic PDE on a time-invariant spatial domain and applied KL decomposition to obtain the set of eigenfunctions on the fixed domain. In application, they used this method in the nonlinear feedback[29] and robust[30] control of one-dimensional (1-D) reaction-diffusion systems. This approach cannot be used in general, since the mathematical transformation does not always have the analytical form, e.g., for nontrivial geometry. To obtain a reduced-order approximation of systems governed by PDEs that have a traveling wave solution, Glavaski and coworkers[31] processed the available dataset using a "centering" procedure prior to performing KL. This procedure involves giving an appropriate definition of the center of a wave and moving it to a standard position. In the contribution by Fogleman et al.[32] the proper orthogonal decomposition (POD) is applied to obtain the phase invariant POD modes of internal combustion engine flows. In their contribution, the velocity fields are stretched in one dimesion to obtain data on a fixed grid such that the divergence-free (continuity) property of the original velocity field is preserved.

Following these ideas, a systematic approach is proposed to obtain a set of empirical eigenfunctions of a set of data given on a spatially time-dependent domain that captures the most energy of the system's dynamics while preserving some physical invariant property. We propose the following methodology which will be discussed in detail in the consecutive sections:

1. The solution to the parabolic PDE can be found as raw data by the experiments or high fidelity numerical simulations which describe the time evolution of dissipative distributed parameter system on a time-varying domain.

2. Geometrically, a mapping can be found by which the time-varying domain of the PDE is transformed to a fixed reference configuration for all times during the evolution of the solutions.

3. Having the set of solutions, the main idea is to transform them to the reference configuration and then use them with the KL decomposition. Among all transformations, the one that preserves the space-invariant property of the PDE solutions is selected. While this mapping transforms data, the mapping introduced in Step 2 transforms geometry of the PDE domain.

4. Then, KL decomposition is applied on the mapped solutions to extract a low-dimensional set of eigenfunctions that contains most of the energy of the system on the fixed domain.

5. Using the inverse of the transformation found in Step 3, these eigenfunctions are mapped on the time-varying domain. As a result, a set of time-varying empirical eigenfunctions are obtained and can be used as a tool for the reduced-order representation of the initially given distributed parameter system.

Along the previous contribution of Izadi and Dubljevic,[33] the focus of this study is to explore this methodology and apply it to more realistic problems, and the examples provided here show the efficiency of the proposed methodology. Also, we point out that domain boundary evolution knowledge is essential in this approach.

Mathematical Formulation

In this section, the mathematical aspects of the proposed method are reviewed. In particular, the mapping that transforms data from time-varying domain to the reference geometry and preserves the properties of the data is derived. A brief essence of the KL decomposition as the representation of a set of stochastic data with minimum number of degrees of freedom is given as well.

Description of the PDE system

The parabolic PDE systems are considered in this work with the following form

$$\frac{\partial x(\xi,t)}{\partial t}=\mathscr{L}(x(\xi,t))+h(x(\xi,t),t)+b(\xi,t)u(t) \tag{1}$$

defined on the time-varying spatial domain $\Omega(t)\subset\mathbb{R}^n$ of the process subject to boundary conditions of the form

$$C_i x(\xi,t)+D_i\mathbf{n}\cdot\nabla x(\xi,t)=R_i \quad \text{on} \quad \Gamma_i(t) \tag{2}$$

and initial condition

$$x(\xi,0)=x_0(\xi) \tag{3}$$

Here, $x(\xi,t)$ is the state variable, $\xi\in\Omega(t)$ is spatial coordinate, $t\in[0,\infty)$ is time, $\mathscr{L}(x(\xi,t))$ is the (nonlinear) differential operator and $h(x(\xi,t),t)$ and $b(\xi,t)$ are smooth functions describing reaction and distribution of the control action $u(t)$, respectively. C_i's, D_i's, and R_i's are constants

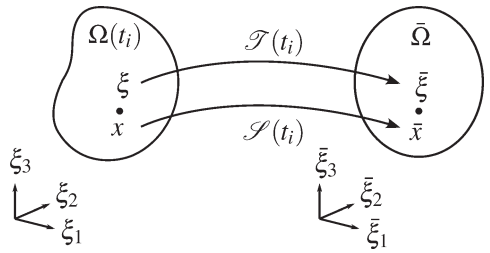

Figure 1. At each time instance t_i, $\mathscr{T}(t_i)$ maps time-varying domain Ω to fixed domain $\bar{\Omega}$.

Also, the transformation $\mathscr{S}(t_i)$ maps the state $x(\xi, t_i)$ from time-varying domain to $\bar{x}_i(\bar{\xi})$ on the fixed domain.

characterizing boundary conditions and $\Gamma_i(t)$'s are portions of the time-varying boundary of $\Omega(t)$. It is assumed that the evolution of domain $\Omega(t)$ is smooth and known *a priori*, as it can be easily measured in many process systems (e.g., phase change in the crystal growth processes). Furthermore, we assume that the solutions of the nonlinear PDE are unique and sufficiently smooth.

Geometry and data transformations

It is intended to obtain a set of time-varying empirical eigenfunctions $\{\phi_j(\xi,t)\}, j=1,2,\cdots,M$ that capture the most energy of the ensemble of solutions (snapshots) $\{x(\xi,t_i)\}, i=1,2,\cdots,N \gg M$ of the parabolic PDE under consideration. The fact that eigenfunctions are inherently time-varying is due to their spatially time-dependent domain.

Suppose that there exists invertible mapping $\mathscr{T}(t)$ which is smooth and preserves orientation of the coordinate system, that maps the domain $\Omega(t)$ to a fixed reference configuration $\bar{\Omega}$ as $\mathscr{T}(t): \xi \in \Omega(t) \mapsto \bar{\xi} \in \bar{\Omega}$ at each time t as shown in Figure 1, with the coordinate transformation $\bar{\xi}=\bar{\xi}(\xi,t)$ and the Jacobian matrix $[J(t)]=\frac{\partial \bar{\xi}}{\partial \xi}$.

Consider the extensive property

$$G(t)=\int_{\Omega(t)} g(x(\xi,t))d\Omega \tag{4}$$

Since the KL decomposition deals with the ensemble of snapshots of solutions of the PDE, we restrict our derivation on the solutions $x(\xi,t_i)$ at time instances $t=t_i, i=1,2,\cdots,N$. In addition, the spatial integral in Eq. 4 allows to parameterize the independent variable time t and associate differential elements $d\Omega=J_i^{-1}d\bar{\Omega}$ at $t=t_i$, where J_i^{-1} is the determinant of the inverse of $[J(t_i)]$. Given the state $x(\xi,t_i)$, we are interested to find $\bar{x}_i(\bar{\xi})$ at each point in $\bar{\Omega}$ such that the property $g(x)$ (e.g., thermal energy or density) is invariant and, therefore, preserved by the following relation

$$g(x(\xi,t_i))d\Omega=g\left(\bar{x}_i(\bar{\xi})\right)d\bar{\Omega} \tag{5}$$

Using the Jacobian of transformation

$$g(x(\xi,t_i))d\Omega=g(x(\xi,t_i))J_i^{-1}d\bar{\Omega} \tag{6}$$

and comparing Eqs. 5 and 6

$$g(x(\xi,t_i))J_i^{-1}=g\left(\bar{x}_i(\bar{\xi})\right) \tag{7}$$

one obtains the state $\bar{x}_i(\bar{\xi})$ in fixed domain as a function of the state in the time-varying domain

$$\bar{x}_i(\bar{\xi})=g^{-1}\left(g(x(\xi,t_i))J_i^{-1}\right) \tag{8}$$

Therefore, Eq. 8 can be regarded as the transformation $\mathscr{S}(t_i)$ that maps the state $x(\xi,t_i)$ on the time-varying domain to the state $\bar{x}_i(\bar{\xi})$ on the fixed reference domain preserving the invariant property $g(x)$. Note that, $\mathscr{T}(t_i)$ maps the domain (geometry) of interest at $t=t_i$, while $\mathscr{S}(t_i)$ maps the state (see Figure 1).

Remark. *The mapping transformation $\mathscr{T}(t_i)$ is required to be nonsingular for all $\xi \in \Omega(t_i)$, that is, the Jacobian being nonzero. This notion comes from the topological characteristics of continuous transformation of domain from one configuration to another. If the transformation preserves the topology of the time-varying domain, the same approach can be used and numerically realized, see numerical simulations section. In the most general case when the time-varying domain contains holes, that is the case of a not simply connected domain, which is mapped into similar topological fixed domain with the holes, the expression given in Eqs. 6–8 holds. On the contrary, if the time-varying domain undergoes topological transformation which implies the change from non-simply connected to more complex connected region (the generation of holes within the domain by continuous transformation), the mapping into the fixed domain configuration will induce additional terms to be accounted for in Eqs. 6–8. In this work, we do not explore these complex cases, since the physical examples explored in our study do not show this type of the time-varying domain transformation.*

KL decomposition

The KL decomposition is a procedure for representation of a stochastic field with a minimum number of degrees of freedom.[34,35] In this subsection, we briefly outline the KL procedure which is used to calculate the empirical eigenfunctions from the data on the fixed domain.

Consider the space of square integrable real-valued functions $\bar{x}(\bar{\xi})$ with inner product $\langle \bar{x}, \bar{y} \rangle$. Given an ensemble of states $\{\bar{x}_i(\bar{\xi})\}, i=1,2,\cdots,N$, whose ensemble average is denoted by

$$\widehat{\bar{x}_i(\bar{\xi})}=\frac{1}{N}\sum_{i=1}^{N}\bar{x}_i(\bar{\xi}) \tag{9}$$

it is intended to obtain a function $\bar{\phi}(\bar{\xi})$ that maximizes $\langle \bar{\phi}, \bar{x}_i \rangle^2$, i.e., $\bar{\phi}(\bar{\xi})$ is closest to all $\bar{x}_i(\bar{\xi})$. This problem can be expressed as finding $\max_{\bar{\phi}(\bar{\xi})} \lambda$ where

$$\lambda=\frac{\langle \widehat{\bar{\phi}, \bar{x}_i} \rangle^2}{\langle \bar{\phi}, \bar{\phi} \rangle} \tag{10}$$

Defining the two-point correlation function $K(\bar{\xi},\bar{\eta})=\widehat{\bar{x}_i(\bar{\xi})\bar{x}_i(\bar{\eta})}$ for $\bar{\xi},\bar{\eta} \in \bar{\Omega}$ and the linear operator $\mathscr{R}$ as

$$\mathscr{R}\bar{\phi}=\langle K(\bar{\xi},\bar{\eta}), \bar{\phi}(\bar{\eta}) \rangle$$

Equation 10 reduces to the following operator eigenvalue problem

$$\mathscr{R}\bar{\phi}=\lambda\bar{\phi} \tag{11}$$

Equation 11 can be solved using the Schmidt–Hilbert technique or the method of snapshots.[36] In this method, the eigenfunction $\bar{\phi}(\bar{\xi})$ is assumed to be a linear combination of ensemble elements as

$$\bar{\phi}(\bar{\xi})=\sum_{i=1}^{N}\alpha_i\bar{x}_i(\bar{\xi}) \tag{12}$$

Replacing Eq. 12 and introducing $P_{ij}=\frac{1}{N}\langle\bar{x}_i(\bar{\eta}),\bar{x}_j(\bar{\eta})\rangle$, Eq. 11 takes the following form

$$\sum_{i=1}^{N}\sum_{j=1}^{N}\bar{x}_i(\bar{\xi})P_{ij}\alpha_j=\lambda\sum_{i=1}^{N}\alpha_i\bar{x}_i(\bar{\xi}) \tag{13}$$

For this to hold, the coefficient of $x_i(\bar{\xi})$ on the left and right hand side of this equation should be equal for all $i=1,2,\cdots,N$, that is

$$\sum_{j=1}^{N}P_{ij}\alpha_j=\lambda\alpha_i \tag{14}$$

which is the eigenvalue problem of the matrix with elements P_{ij}. Finally, the set of eigenfunctions $\bar{\phi}_i(\bar{\xi}), i=1,2,\cdots,M$ associated with the M largest eigenvalues of $\mathscr{R}$ forms an optimal basis in the sense of $\bar{x}(\bar{\xi})$ representation in terms of $\bar{\phi}_i(\bar{\xi})$ with minimum error.

Remark. *The size of matrix P is as large as the number of snapshots of the PDE solution. On the other hand, for a set of eigenfunctions to be able to approximate the solutions accurately, the ensemble of solutions should contain adequate number of snapshots. Therefore, one faces the issue of a large matrix eigenvalue problem and numerical methods suitable for these problems. In this work, Arnoldi algorithm is used to solve the large matrix eigenvalue problem to reduce computational costs.*

Time-varying empirical eigenfunctions

Once the set of M eigenfunctions $\bar{\phi}(\bar{\xi})$ are found, they can be transformed to the time-varying domain Ω at each time t_i using the inverse of $\mathscr{S}(t_i)$ (see Eq. 8). Therefore, we have the basis of M time-varying eigenfunctions $\phi(\xi,t)$ which can be used to represent the state $x(\xi,t)$ on the time-varying domain $\Omega(t)$.

Numerical Simulations

In this section, the proposed methodology is applied to three different PDE systems. For the first two process examples, the evolution of the systems is obtained as a solution of nonlinear parabolic PDEs by using the Galerkin's method, whereas for the third system, a moving-mesh finite element realization is developed. It is emphasized that domain evolution is known *a priori* in these simulation studies. In the subsequent numerical procedure, the eigenfunctions $\bar{\phi}_i(\bar{\xi})$ obtained from the method of snapshots are orthogonal and they are normalized to generate an orthonormal basis.

Model formulation of PDE systems with time-dependent domain

This section is devoted to formulate the dynamics of a diffusion-reaction process with time-varying domain using continuum mechanics tools. In particular, we are interested in the model dynamics of an extensive property

$$G(t)=\int_{\Omega(t)}\rho(\xi,t)Cx(\xi,t)d\Omega \tag{15}$$

given by the intensive property $x(\xi,t)$ at each point $\xi\in\Omega(t)\subset\mathbb{R}^n$, where $\rho(\xi,t)$ is density and C is a constant. The body under consideration has the velocity $\mathbf{v}(\xi,t)$ and the boundary $\Gamma(t)$ of the domain $\Omega(t)$ has the velocity $\mathbf{v}_s(\xi|_{\Gamma(t)},t)$, see Figure 2.

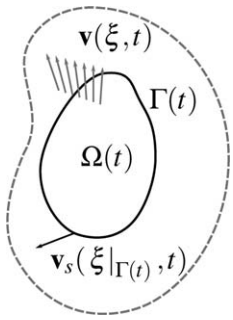

Figure 2. The control volume $\Omega(t)$ is a part of the body with velocity $\mathbf{v}(\xi,t)$.

The boundary $\Gamma(t)$ of the control volume has the velocity $\mathbf{v}_s$.

The total change of $G(t)$ in the domain $\Omega(t)$ is given by the Leibniz integral rule for multidimensions[37] as follows

$$\frac{d}{dt}\int_{\Omega}\rho Cxd\Omega=\int_{\Omega}\frac{\partial}{\partial t}(\rho Cx)d\Omega+\int_{\Gamma}\mathbf{n}\cdot\mathbf{v}_s\rho Cxd\Gamma \tag{16}$$

where $\mathbf{n}$ is the normal outward vector at each point on the Γ. On the other hand, conservation of the property $G(t)$ yields

$$\begin{aligned}\frac{d}{dt}\int_{\Omega}\rho Cxd\Omega&=\int_{\Gamma}\mathbf{n}\cdot\kappa\nabla xd\Gamma\\&\quad-\int_{\Gamma}\mathbf{n}\cdot(\mathbf{v}-\mathbf{v}_s)\rho Cxd\Gamma+\int_{\Omega}(h+bu)d\Omega\end{aligned} \tag{17}$$

where κ is diffusivity and $h(x(\xi,t),t)$ and $b(\xi,t)$ are smooth functions describing internal reaction/generation and distribution of the control action $u(t)$. This equation states that the total change in the property $G(t)$ is given by the difference in the diffusive flux and mass transport from the boundary, in addition to internal generation and external input. Substituting Eq. 16 on the left-side of Eq. 17 and using divergence theorem leads to the following differential form of the governing equation

$$\frac{\partial}{\partial t}(\rho Cx)=\nabla\cdot(\kappa\nabla x-\mathbf{v}\rho Cx)+h+bu \tag{18}$$

For $x=C=1$ and the assumption of constant density, this equation reduces to the continuity as $\nabla\cdot\mathbf{v}=0$. Then, the differential form becomes

$$\rho C\frac{\partial x}{\partial t}=\nabla\cdot(\kappa\nabla x)-\rho C\mathbf{v}\cdot\nabla x+h+bu \tag{19}$$

This equation describes the differential form of a diffusion-reaction process dynamics in terms of the property $x(\xi,t)$ in the time-varying domain $\Omega(t)$.

1-D nonlinear reaction-diffusion system

Consider the 1-D reaction-diffusion system described by the following parabolic PDE

$$\frac{\partial x(\xi,t)}{\partial t}=k\frac{\partial^2x(\xi,t)}{\partial\xi^2}-\dot{l}(t)\frac{\partial x(\xi,t)}{\partial\xi}+h(x(\xi,t)) \tag{20}$$

on the time-varying domain $l(t)=\pi(1.4-0.4e^{-0.74t})$, $\dot{l}(t)=dl(t)/dt$, subject to Dirichlet boundary conditions

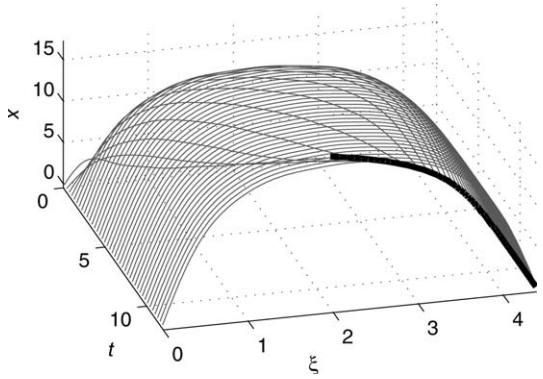

Figure 3. Evolution of the state of 1-D PDE given by Eqs. 20–22 obtained from Galerkin's method using 10th-order sinusoidal model.

Thick black line shows domain evolution.

$$x(0,t)=0, x(l(t),t)=0 \tag{21}$$

and initial condition $x(\xi,0)=x_0(\xi)$. The process can be considered as the 1-D approximation of temperature evolution $x(\xi,t)$ in a catalytic rod. The reaction term is given by

$$h(x)=\beta_1\left(e^{-\frac{\gamma}{1+x}}-e^{-\gamma}\right)-\beta_2 x \tag{22}$$

This example is adopted from Ref. 29 where nondimensional process parameters k and β_2 are functions of space ξ. For simplicity, we averaged these parameters over domain and used $k=0.4, \beta_1=45, \beta_2=2$, and $\gamma=4$, however, the approach can be generalized for parameters depending on spatial coordinates.

To obtain an ensemble of solutions of Eq. 20, the Galerkin's method with the set of orthonormal basis functions

$$\psi_i(\xi,t)=\sqrt{\frac{2}{l(t)}}\sin\left(\frac{i\pi\xi}{l(t)}\right) \tag{23}$$

is used. An explicit Euler integration scheme is utilized to construct a higher-order resolution of the problem. Figure 3 shows the evolution of state of 1-D PDE using 10 modes of the Galerkin's method.

For this example, the reference configuration is simply a 1-D domain with constant length L_0 and the mapping $\mathscr{T}(t_i)$ is given by

$$\bar{\xi}=\frac{L_0}{l(t_i)}\xi \tag{24}$$

If the state $x(\xi,t)$ represents the temperature at $\xi\in\Omega$, the invariant property of interest can be interpreted to be thermal energy $g(x(\xi,t_i))=\rho c_p x(\xi,t_i)$ and from Eq. 8, the mapping $\mathscr{S}(t_i)$ associated with is given as

$$\bar{x}_i(\bar{\xi})=\frac{1}{\rho c_p}\left(\rho c_p x(\xi,t_i)J_i^{-1}\right)=\frac{l(t_i)}{L_0}x(\xi,t_i) \tag{25}$$

Having the temperature distribution $\bar{x}_i(\bar{\xi})$ on the fixed domain $\bar{\Omega}$, one can perform KL decomposition to extract empirical eigenfunctions $\bar{\phi}_j(\bar{\xi}), j=1,2,\cdots,M$ of the data with inner product $\langle\bar{x},\bar{y}\rangle=\int_0^{L_0}\bar{x}\bar{y}d\bar{\xi}$. Figure 4a shows the first three eigenfunctions on the fixed domain. Time-varying eigenfunctions are obtained by using the inverse mapping $\mathscr{S}^{-1}$ and the first two of them are shown in Figure 4b.

The set of time-varying eigenfunctions are used in the Galerkin's method to obtain the reduced-order model by replacing $x(\xi,t)=\sum_{i=1}^{M}a_i(t)\phi_i(\xi,t)$ in Eq. 20 to get

$$\sum_{i=1}^{M}\left(\dot{a}_i\phi_i+a_i\dot{\phi}_i\right)=\sum_{i=1}^{M}\left(ka_i\phi_i''-\dot{l}a_i\phi_i'\right)+h\left(\sum_{i=1}^{M}a_i\phi_i\right) \tag{26}$$

where over dot and prime represent derivatives with respect to time and space, respectively. Projecting on the basis ϕ_j yields

$$\dot{a}(t)=A(t)a(t)+\bar{h}(a(t),t) \tag{27}$$

where $a(t)=[a_1(t)a_2(t)\cdots a_M(t)]^T, A_{ij}(t)=\frac{\langle k\phi_i''-\dot{l}\phi_i'-\dot{\phi}_i,\phi_j\rangle}{c(t)}$, $\bar{h}_j(a_i(t),t)=\frac{\left\langle h\left(\sum_{i=1}^{M}a_i\phi_i\right),\phi_j\right\rangle}{c(t)}$, and $c(t)=[L_0/l(t)]^2$.

Equation 27 represents the reduced-order model of the Eq. 20. Figure 5 compares the evolution of the norm of the states $||x||=\langle x,x\rangle^{1/2}$ for reconstruction of Figure 3 with three time-varying eigenfunctions used in Eq. 27. As it can be seen from Figure 5, the reduced-order model almost perfectly matches the profile obtained from the high-order fidelity simulation.

Remark. *The set of eigenfunctions ϕ_i in this example are orthogonal and $\langle\phi_i(\xi,t),\phi_j(\xi,t)\rangle=c(t)\delta_{ij}$ with δ_{ij} being Kronecker's delta. This is because the determinant of the Jacobian is not spatial-dependent. For general transformation in multidimensions, this condition does not hold (see the 2-D linear diffusive system with nontrivial geometry example).*

2-D nonlinear reaction-diffusion system

The second example is the 2-D reaction-diffusion system governed by the nonlinear parabolic PDE given by

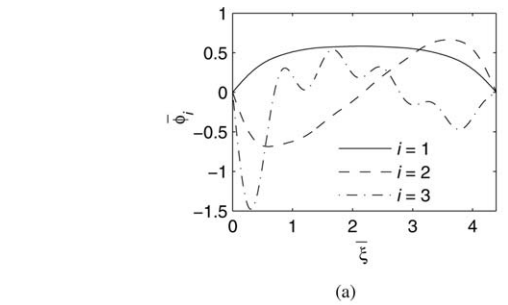

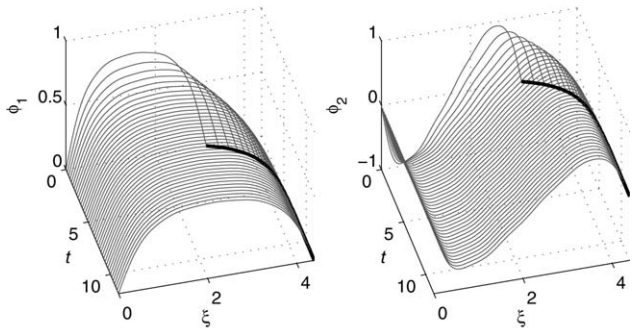

Figure 4. (a) The first three eigenfunctions extracted from the data mapped to the fixed domain; (b) the first two time-varying eigenfunctions.

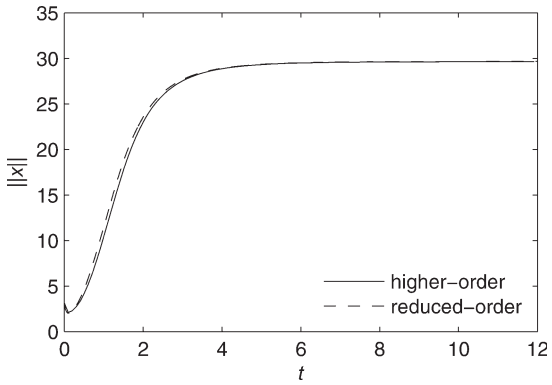

Figure 5. Comparison of the norm of the state for higher-order and reduced-order resolutions of the 1-D PDE.

$$\frac{\partial x(\xi_1,\xi_2,t)}{\partial t}=k\nabla^2 x(\xi_1,\xi_2,t)+h(x(\xi_1,\xi_2,t))+u(t) \tag{28}$$

on the time-varying rectangular domain $L_1(t)\times L_2(t)\in\mathbb{R}^2$ subject to Dirichlet boundary conditions

$$x(0,\xi_2,t)=x(L_1(t),\xi_2,t)=x(\xi_1,0,t)=x(\xi_1,L_2(t),t)=0 \tag{29}$$

and initial condition $x(\xi_1,\xi_2,0)=x_0(\xi_1,\xi_2)$, see Figure 6. The reaction term and process parameters are the same as in the previous example and $u(t)$ is the input. The ensemble of solutions of Eq. 28 subjected to the input shown in Figure 8a is obtained using the Galerkin's method with the set of orthogonal basis functions

$$\psi_{ij}(\xi_1,\xi_2,t)=\sin\left(\frac{i\pi\xi_1}{l_1(t)}\right)\sin\left(\frac{j\pi\xi_2}{l_2(t)}\right) \tag{30}$$

The reference fixed configuration $\bar{\Omega}$ on which the solutions of Eq. 28 are mapped is considered to be a square with lengths $L_0=4$, then the Jacobian matrix of transformation $\mathscr{T}(t_i)$ is

$$J(t_i)=\begin{bmatrix}\dfrac{L_0}{L_1(t_i)} & 0\\ 0 & \dfrac{L_0}{L_2(t_i)}\end{bmatrix} \tag{31}$$

Using the same energy function $g(x)=\rho c_p x$ as in the previous example, from Eq. 8 we map the ensemble of solutions to the fixed domain to obtain the dataset for the KL

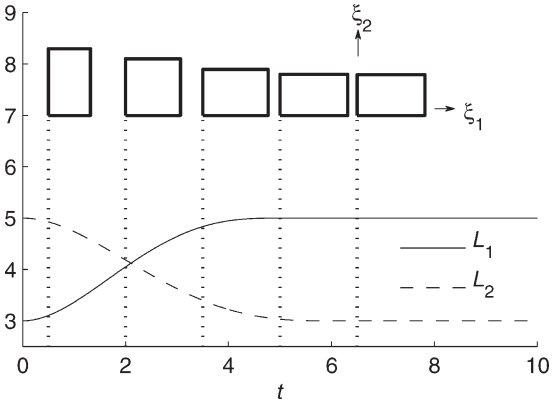

Figure 6. 2-D time-varying domain of the nonlinear diffusion-reaction system.

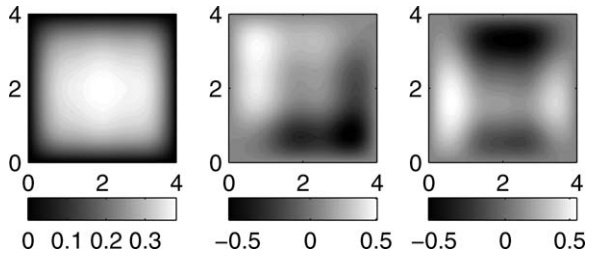

Figure 7. The first three eigenfunctions extracted from the data mapped to the fixed domain for the 2-D nonlinear PDE.

decomposition. The first three extracted empirical eigenfunctions are shown in Figure 7.

These eigenfunctions are mapped on the time-varying domain at each time instance t_i to obtain the set of time-varying empirical eigenfunctions. Using this set in the Galerkin's method, the state evolution can be reconstructed. Figure 8b shows the evolution of the norm of states for simulations based on 25 sinusoidal function space basis and 3 empirical eigenfunctions.

2-D linear diffusive system with nontrivial geometry

In this section, the proposed methodology is applied to a diffusive process where the geometry of the time-varying domain is nontrivial. The Jacobian matrix of transformation in this case is not only time-dependent, but also it is space dependent, which implies that the Jacobian matrix needs to be computationally determined for each point within the deformable domain.

We consider the 2-D axisymmetric diffusive system described by the following parabolic PDE

$$\frac{\partial x}{\partial t}=k\left[\frac{1}{r}\frac{\partial}{\partial r}\left(r\frac{\partial x}{\partial r}\right)+\frac{\partial^2 x}{\partial z^2}\right]-\dot{L}\frac{\partial x}{\partial z}+u \tag{32}$$

for $x(r,z,t)$ in the time-varying domain $\Omega(t)$ shown in Figure 9a, subject to boundary conditions

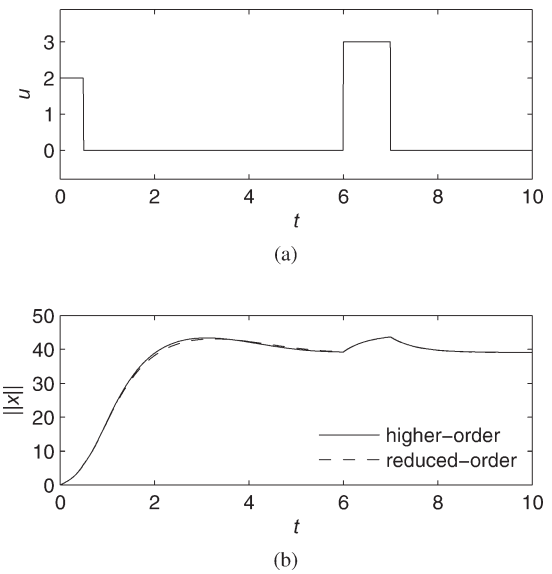

Figure 8. (a) Input to the 2-D reaction diffusion system. (b) Comparison of the norm of the state for higher-order and reduced-order resolutions of the 2-D PDE.

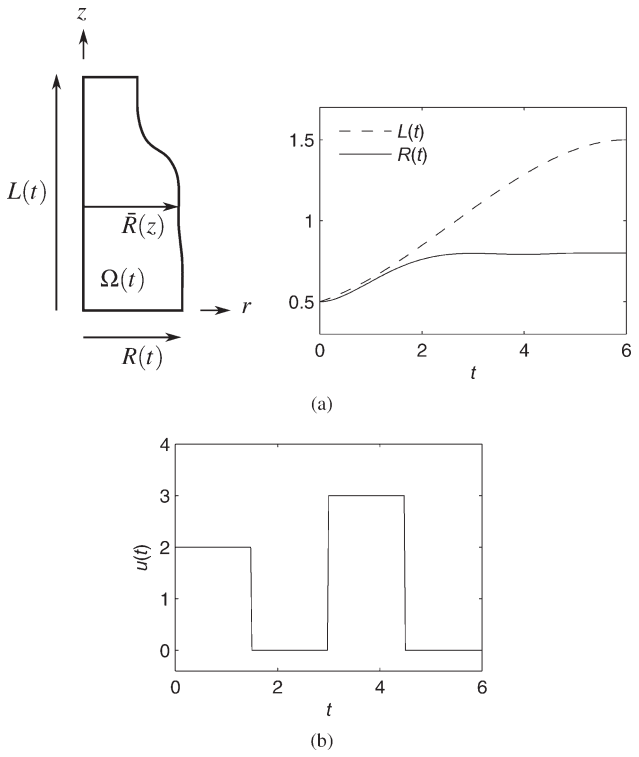

Figure 9. (a) Schematic representation of crystal growth in the 2-D Czochralski process given by Eqs. 32 and 33.

***L*(*t*) and *R*(*t*) are the length and radius of crystal at time *t*. (b) The heat input to the Czochralski system.**

$$x(r,0,t)=x(r,L(t),t)=0$$
$$\left.\frac{\partial x(r,z,t)}{\partial r}\right|_{r=0}=\left.\frac{\partial x(r,z,t)}{\partial r}\right|_{r=\bar{R}(z)}=0 \tag{33}$$

with nondimensional process parameter $k=0.25$ and $\dot{L}(t)$ represents derivative of the length function $L(t)$ with respect to time. This system is a model that describes the nondimensionalized crystal temperature distribution in the Czochralski crystal growth process. In this method, the crystal rod is pulled out vertically from the surface ($z=0$) of a heated pool of melt contained in a crucible. A simplified radius control strategy arising from geometric model provides the domain evolution in terms of $L(t)$ and $R(t)$ as shown in Figure 9a, and $u(t)$ is the heat input to the parabolic PDE system.

The ensemble of solution of Eq. 32 is obtained using the finite element method. Since the geometry of domain is time-varying, a mesh moving scheme is used. Due to the fact that the evolution of the domain is not coupled with the PDE system (Eq. 32) and is known, the arbitrary Lagrangian

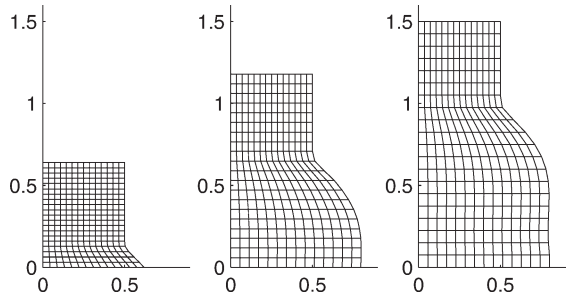

Figure 10. Finite element moving mesh at $t=1, 3.5$, and, 6.

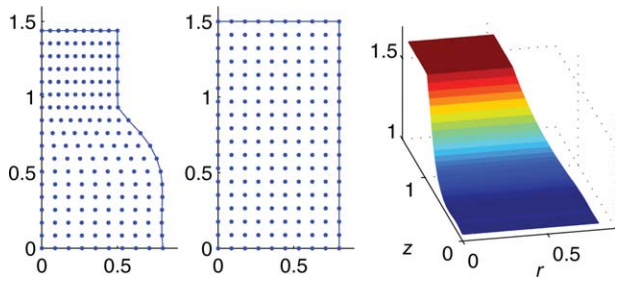

Figure 11. The sets of 10 × 18 grid points in time-varying domain at $t=5$ (left panel) and in the fixed domain (middle panel).

These computational grid points define the mapping $\mathcal{T}(t_i)$ by associating each point of the time-varying domain with one point in the fixed domain. Right panel shows $J_i^{-1}(r,z)$ at $t_i=5$.

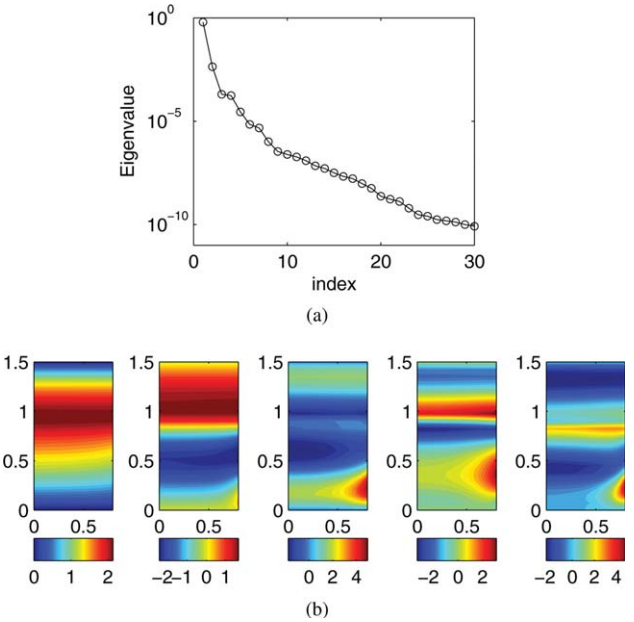

Figure 12. (a) The first 30 eigenvalues of the KL decomposition; (b) the first five eigenfunctions extracted from the data mapped to the fixed domain.

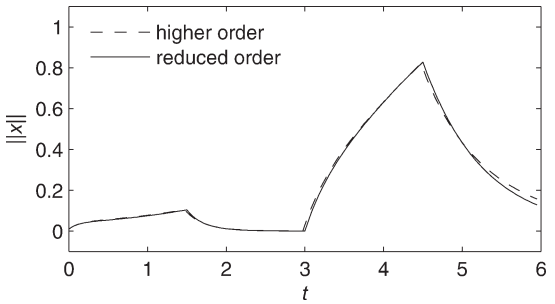

Figure 13. Comparison of the norm of the state for the higher-order finite element and reduced-order Galerkin's method resolutions of the parabolic PDE.

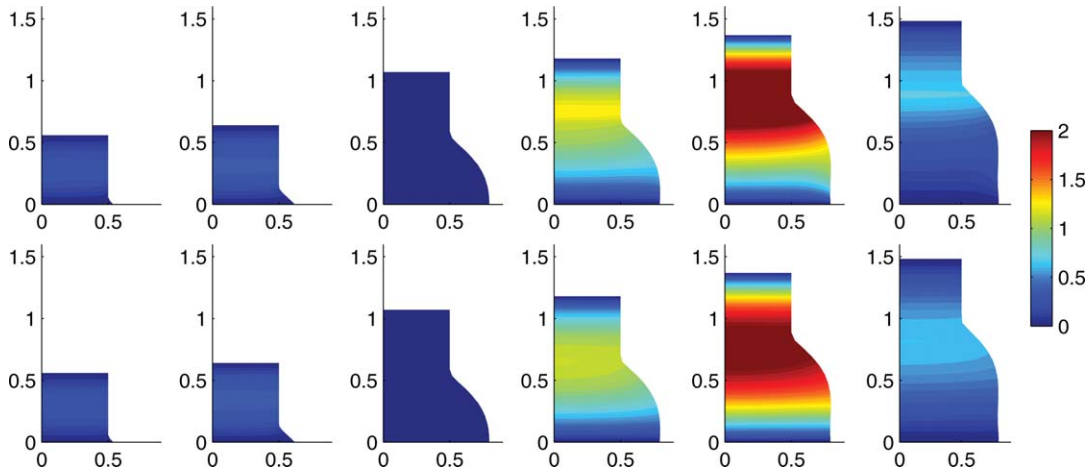

Figure 14. Solution of the 2-D diffusion-reaction system with the time-dependent spatial domain using the higher-order finite element (top) and reduced-order (bottom) model at $t = 0.5$, 1, 3, 4, 4.5, and 5.5.

Eulerian method[38] is used to spatially discretize domain of interest as shown in Figure 10. The finite element mesh consists of 14 × 20 2-D linear four-node elements which discretizes spatial geometry to 285 degrees of freedom. The evolution of the time-dependent set of ordinary differential equations obtained from the finite element discretization is realized by first-order implicit time integration with the time step $dt=0.025$, while the heat input $u(t)$ is an arbitrary constructed function shown in Figure 9b.

To apply the proposed methodology, the reference configuration $\bar{\Omega}$ on which the solutions of Eq. 32 are mapped is considered to be a rectangle with dimensions $\bar{R}=0.8$ and $\bar{L}=1.5$. The mapping $\mathscr{T}(t_i)$ can be numerically constructed by introducing sets of computational grid points on both time-varying and fixed domains, as shown in Figure 11. Associating each grid point of the time-varying domain with one and only one grid point on the fixed-domain defines the one-to-one and onto (and hence invertible) mapping $\mathscr{T}(t_i)$. Note that, the coarse grid of 10 × 18 points is shown in Figure 11 for illustration and we used 40 × 80 grid points for calculation of the Jacobian. Also, it is important to emphasize that the Jacobian matrix of transformation in this case is space-dependant.

Considering the state $x(r,z,t)$ as temperature at $(r,z)\in\Omega(t)$, the invariant property $g(x(\xi,t_i))$ can be considered to be thermal energy as in previous examples and from Eq. 8, the map $\mathscr{S}(t_i)$ found as

$$\bar{x}_i(\bar{r},\bar{z})=J_i^{-1}x(r,z,t_i) \tag{34}$$

Having the temperature distribution $\bar{x}_i(\bar{r},\bar{z})$ on the fixed domain $\bar{\Omega}$, one can perform KL decomposition to extract empirical eigenfunctions $\bar{\phi}_j(\bar{r},\bar{z}), j=1,2,\cdots,M$ of the data with inner product defined as

$$\langle\bar{x},\bar{y}\rangle=\int_{\bar{\Omega}}\bar{r}\bar{x}\bar{y}d\bar{r}d\bar{z} \tag{35}$$

Figure 12a shows the first 30 eigenvalues of the KL decomposition (see Eq. 11), the first mode captures 99.2% of the energy solutions. Figure 12b shows the first five eigenfunctions on the fixed domain.

The use of $\mathscr{S}^{-1}$ on eigenfunctions extracted from the data mapped to the reference configuration results in the time-varying eigenfunctions. Then, the Galerkin's method is used to obtain the reduced-order model by replacing $x(r,z,t)=\sum_{i=1}^{M}a_i(t)\phi_i(r,z,t)$ in Eq. 32 and projecting on the basis ϕ_j to get

$$\dot{a}(t)=A(t)a(t)+B(t)u(t) \tag{36}$$

where

$$\begin{aligned}
a(t) &= [a_1(t)a_2(t)\cdots a_M(t)]^T\\
A(t) &= C(t)^{-1}K(t), B=C(t)^{-1}F(t)\\
C_{ij}(t) &= \langle\phi_i,\phi_j\rangle\\
K_{ij}(t) &= \left\langle k\left[\frac{1}{r}\frac{\partial}{\partial r}\left(r\frac{\partial\phi_i}{\partial r}\right)+\frac{\partial^2\phi_i}{\partial z^2}\right]-\dot{L}\frac{\partial\phi_i}{\partial z}-\frac{\partial\phi_i}{\partial t},\phi_j\right\rangle\\
F_i(t) &= \langle 1,\phi_i\rangle
\end{aligned} \tag{37}$$

Equation 36 represents the reduced-order form of Eq. 32.

Figure 13 compares the evolution of the norm of the states for reconstruction of the solutions of Eq. 32 with the same input with two time-varying eigenfunctions used in Eq. 36. As it can be seen, the reduced-order model perfectly matches the profile obtained from the high-order simulation, the finite element model with order of 285 is reduced to a second-order system. Reconstructed states resulting from the reduced-order model are shown in Figure 14 against the finite element solutions.

Conclusions

In this article, we proposed a method to obtain a set of time-varying empirical eigenfunctions of a set of data given on the spatially time-dependent domain. In this method, the solutions of the PDE system on the time-varying domain are mapped to a fixed reference configuration in such a way that invariant properties of the data are preserved. Then, KL decomposition is applied on the mapped solutions to extract a small set of eigenfunctions that contains most of the energy of system on the fixed domain. These eigenfunctions are mapped back on the time-varying domain yielding a set of time-varying empirical eigenfunctions that can be used as the reduced-order representation of the main PDE system.

In the simulation part, the procedure is applied to two nonlinear reaction-diffusion systems with trivial domain, as well as a 2-D axisymmetric problem of temperature distribution of the Czochralski crystal growth process governed by parabolic PDE which represents time-varying domain with nontrivial geometry. The results show the capability of the method as a useful and efficient tool in representations of the reduced-order system with the time-varying domain.

Acknowledgment

Financial support by Natural Science and Engineering Research Council of Canada (NSERC) Discovery Grant 386508-2011 is gratefully acknowledged.

Literature Cited

1. Wang PKC. Stabilization and control of distributed systems with time-dependent spatial domains. *J Optim Theory Appl*. 1990;65(2): 331–362.
2. Wang PKC. Feedback control of a heat diffusion system with time-dependent spatial domain. *Optim Control Appl Methods*. 1995;16(5): 305–320.
3. Ray WH, Seinfeld JH. Filtering in distributed parameter systems with moving boundaries. *Automatica*. 1975;11(5):509–515.
4. Ng J, Dubljevic S. Optimal control of convection-diffusion process with time-varying spatial domain: Czochralski crystal growth. *J Process Control*. 2011;21(10):1361–1369.
5. Ng J, Dubljevic S. Optimal boundary control of a diffusion-convection-reaction PDE model with time-dependent spatial domain: Czochralski crystal growth process. *Chem Eng Sci*. 2012;67(1):111–119.
6. Gay DH, Ray WH. Identification and control of distributed parameter systems by means of the singular value decomposition. *Chem Eng Sci*. 1995;50(10):1519–1539.
7. Chakravarti S, Ray WH. Boundary identification and control of distributed parameter systems using singular functions. *Chem Eng Sci*. 1999;54(9):1181–1204.
8. Park HM, Cho DH. The use of the Karhunen-Loève decomposition for the modeling of distributed parameter systems. *Chem Eng Sci*. 1996;51(1):81–98.
9. Christofides PD. Nonlinear and Robust Control of PDE Systems: Methods and Applications to Transport-Reaction Processes. Birkhäuser, Boston, MA, 2001.
10. Armaou A, Christofides PD. Dynamic optimization of dissipative PDE systems using nonlinear order reduction. *Chem Eng Sci*. 2002; 57(24):5083–5114.
11. Zheng D, Hoo KA. Low-order model identification for implementable control solutions of distributed parameter systems. *Comput Chem Eng*. 2002;26(7):1049–1076.
12. Zheng D, Hoo KA. System identification and model-based control for distributed parameter systems. *Comput Chem Eng*. 2004;28(8): 1361–1375.
13. Park HM, Lee JH. A method of solving inverse convection problems by means of mode reduction. *Chem Eng Sci*. 1998;53(9):1731–1744.
14. Park HM, Lee MW. Boundary control of the Navier–Stokes equation by empirical reduction of modes. *Comput Methods Appl Mech Eng*. 2000;188(1):165–186.
15. Bangia AK, Batcho PF, Kevrekidis IG, Karniadakis GE. Unsteady two-dimensional flows in complex geometries: Comparative bifurcation studies with global eigenfunction expansions. *SIAM J Sci Comput*. 1997;18(3):775.
16. Park HM, Jung WS. The Karhunen-Loève-Galerkin method for the inverse natural convection problems. *Int J Heat Mass Transfer*. 2001;44(1):155–167.
17. Shvartsman SY, Kevrekidis IG. Nonlinear model reduction for control of distributed systems: A computer-assisted study. *AIChE J*. 1998; 44(7):1579–1595.
18. Theodoropoulou A, Zafiriou E, Adomaitis RA. Inverse model-based real-time control for temperature uniformity of RTCVD. *IEEE Trans Semicond Manufact*. 1999;12(1):87–101.
19. Baker J, Christofides PD. Finite-dimensional approximation and control of non-linear parabolic PDE systems. *Int J Control*. 2000;73(5): 439–456.
20. Arkun Y, Kayihan F. A novel approach to full CD profile control of sheet-forming processes using adaptive PCA and reduced-order IMC design. *Comput Chem Eng*. 1998;22(7–8):945 – 962.
21. Raimondeau S, Vlachos D. Low-dimensional approximations of multiscale epitaxial growth models for microstructure control of materials. *J Comput Phys*. 2000;160(2):564–576.
22. Zhou XG, Zhang XS, Wang X, Dai YC, Yuan WK. Optimal control of batch electrochemical reactor using KL expansion. *Chem Eng Sci*. 2001;56(4):1485–1490.
23. Mangold M, Sheng M. Nonlinear model reduction of a two-dimensional MCFC model with internal reforming. *Fuel Cells*. 2004; 4(1–2):68–77.
24. Bleris LG, Kothare MV. Reduced order distributed boundary control of thermal transients in microsystems. *IEEE Trans Control Syst Technol*. 2005;13(6):853–867.
25. Nie Q, Joshi Y. Multiscale thermal modeling methodology for thermoelectrically cooled electronic cabinets. *Numer Heat Transfer Part A: Appl*. 2008;53(3):225–248.
26. McPhee J, Yeh W. Groundwater management using model reduction via empirical orthogonal functions. *J Water Resour Plann Manage*. 2008;134(2):161–170.
27. Park HM, Lim JY. A reduced-order model of the low-voltage cascade electroosmotic micropump. *Microfluidics Nanofluidics*. 2009; 6(4):509–520.
28. Armaou A, Christofides PD. Computation of empirical eigenfunctions and order reduction for nonlinear parabolic PDE systems with time-dependent spatial domains. *Nonlinear Anal: Theory Methods Appl*. 2001;47(4):2869–2874.
29. Armaou A, Christofides PD. Finite-dimensional control of nonlinear parabolic PDE systems with time-dependent spatial domains using empirical eigenfunctions. *Appl Math Comput Sci*. 2001;11(2):287–318.
30. Armaou A, Christofides PD. Robust control of parabolic PDE systems with time-dependent spatial domains. *Automatica*. 2001;37(1): 61–69.
31. Glavaski S, Marsden JE, Murray RM. Model reduction, centering, and the Karhunen-Loève expansion. In: Proceeding of the 37th IEEE Conference on Decision and Control, December 16–18, 1998, Tampa, FL, published by IEEE in Piscataway, NJ, Vol. 2, 1998: 2071–2076.
32. Fogleman M, Lumley J, Rempfer D, Haworth D. Application of the proper orthogonal decomposition to datasets of internal combustion engine flows. *J Turbulence*. 2004;5:023.
33. Izadi M, Dubljevic S. Computation of empirical eigenfunctions of parabolic PDEs with time-varying domain. In: Proceeding of the 2012 American Control Conference, June 27–29, 2012, Montreal, Canada, published by AACC in Tory, NY, 2012;4357–4362.
34. Loeve M. Probability Theory. Princeton, NJ: Van Nostrand, 1955.
35. Sirovich L, Park H. Turbulent thermal convection in a finite domain: Part I. *Theory. Phys Fluids A: Fluid Dyn*. 1990;2:1649–1658.
36. Sirovich L. Turbulence and the dynamics of coherent structures. I-Coherent structures. II-Symmetries and transformations. III-Dynamics and scaling. *Quart Appl Math*. 1987;45:561–571.
37. Deen WM. Analysis of Transport Phenomena. New York: Oxford University Press, 1998.
38. Reddy JN, Gartling DK. The Finite Element Method in Heat Transfer and Fluid Dynamics. Boca Raton, FL: CRC, 2010.

Manuscript received Dec. 30, 2012, and revision received May. 10, 2013.